university of groningen

umcg

University of Groningen

# Chromism of spiropyrans

Kortekaas, Luuk

**IMPORTANT NOTE: You are advised to consult the publisher's version (publisher's PDF) if you wish to cite from it. Please check the document version below.**

*Document Version*
Publisher's PDF, also known as Version of record

*Publication date:*
2018

Link to publication in University of Groningen/UMCG research database

*Citation for published version (APA):*
Kortekaas, L. (2018). *Chromism of spiropyrans: from solutions to surfaces*. [Thesis fully internal (DIV), University of Groningen]. University of Groningen.

**Copyright**
Other than for strictly personal use, it is not permitted to download or to forward/distribute the text or part of it without the consent of the author(s) and/or copyright holder(s), unless the work is under an open content license (like Creative Commons).

The publication may also be distributed here under the terms of Article 25fa of the Dutch Copyright Act, indicated by the "Taverne" license. More information can be found on the University of Groningen website: https://www.rug.nl/library/open-access/self-archiving-pure/taverne-amendment.

**Take-down policy**
If you believe that this document breaches copyright please contact us providing details, and we will remove access to the work immediately and investigate your claim.

*Downloaded from the University of Groningen/UMCG research database (Pure): http://www.rug.nl/research/portal. For technical reasons the number of authors shown on this cover page is limited to 10 maximum.*

Download date: 13-07-2025

# Chapter 4

# A Remarkable Multitasking Double Spiropyran: Bidirectional Visible-Light Switching of Polymer-Coated Surfaces with Dual Redox and Proton Gating

**Abstract** Smart or functional surfaces that exhibit complex multimodal responsivity, e.g., to light, heat, pH, etc., although highly desirable, require a combination of distinct functional units to achieve each type of response and present a challenge in achieving combinations that can avoid cross-talk between the units, such as excited-state quenching. Compounds that exhibit multiple switching modalities help overcome this challenge and drastically reduce the synthetic cost and complexity. Here we show that a bis-spiropyran photochrome, which is formed through coupling at the indoline 5-position using redox chemistry, exhibits pH gated photochromism, with opening of the spiro moiety by irradiation with UV light and the expected reversion by either heating or irradiation with visible light gated by protonation/deprotonation. Remarkably, when the photochrome is oxidized to its dicationic form, bis-spiropyran$^{2+}$, visible light can be used instead of UV light to switch between the spiro and merocyanine forms, with locking and unlocking of each state achieved by protonation/deprotonation. The formation of the bis-spiropyran unit by electrochemical coupling is exploited to generate "smart surfaces", i.e., polymer-modified electrodes, avoiding the need to introduce an ancillary functional group for polymerization and the concomitant potential for cross-talk. The approach taken means not only that the multiresponsive properties of the bis-spiropyran are retained upon immobilization but also that the effective switching rate can be enhanced dramatically.



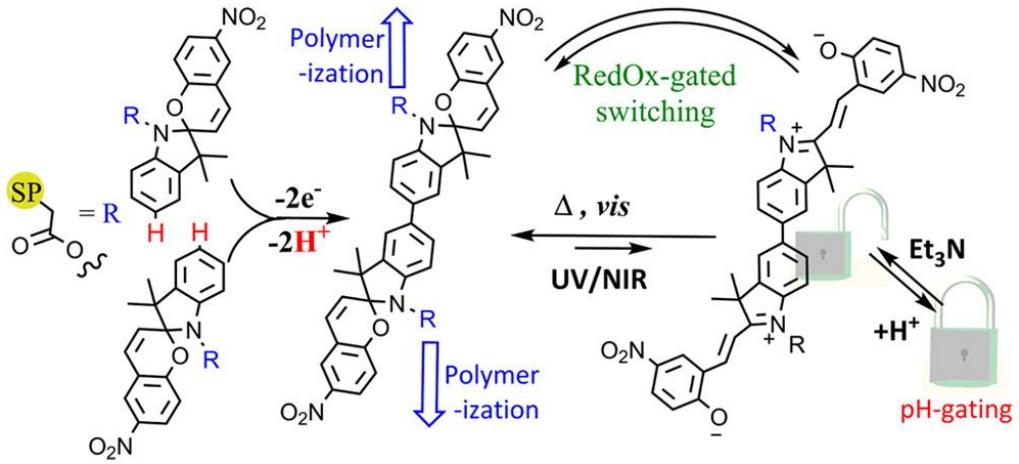


This chapter was published as: L. Kortekaas, O. Ivashenko, J. T. van Herpt and W. R. Browne, *J. Am. Chem. Soc.,* 2016, *138*, 4, 1301-1312. DOI: 10.1021/jacs.5b11604. The Supporting information can be found online.

## Introduction

Surfaces that respond to external stimuli to enable changes in surface properties,[1] such as wettability,[2] adhesion,[3] surface roughness,[4] and biocompatibility,[5] have received widespread interest with applications in fields as diverse as sensor technologies,[6] cell culture,[7] solar management systems[8], fluorescence modulation[9] and electro- and photochromic devices.[10] In particular, surfaces that allow switching of surface properties through external stimuli, have been applied extensively in the control of cell growth through patterning of surfaces not only prior to cell growth but also during the process, which has enabled a deeper understanding in the factors that control cell morphology and growth direction.[11] Furthermore, photoswitchable modified electrodes have been applied extensively, in particular with spiropyrans, to the control of interfacial electron transfer kinetics, as demonstrated elegantly by Katz, Willner, and others.[12] Photo- and redox-switching of surface properties through self-assembled monolayers and polymers is of particular interest, as they offer the possibility of rapid and complete control.[13] These functionalized surfaces are attractive because of the wide range of approaches that can be taken toward their preparation including activated substrates,[14] self-assembly through thiol- or alkylsiloxy-terminated aliphatic chain ends,[15] functionalized polymers,[16] and plasma-induced grafting.[17] Two key challenges faced in introducing responsiveness lie in the requirement for chemical compatibility between the method used for surface modification and the switching unit and, more importantly, the retention of photochromic response after immobilization.[18]

Among the many approaches to surface modification, the in situ electrochemical formation of polymers at electrode surfaces provides a simple yet robust method for obtaining electroactive thin films and has been applied in a number of systems incorporating photochromes such as stilbenes,[19] diarylethenes,[20] and spiropyrans.[21] A challenge presented in using electropolymerization is that it typically requires the addition of a second functional (electropolymerizable) group in addition to the photochromic unit and hence risks "cross-talk" between the functioning of the polymerizable unit and the photoresponsive unit (*vide infra*, Scheme 2). The central challenge is to avoid the loss of photochemical performance after polymerization. For example, in the case of a dithienylperfluorocyclopentene photochromic switch to which two bithiophene units were appended, electropolymerization to form ethene-bridged sexithiophene polymers proceeded smoothly when the monomers were in the colorless open form but was prevented by photochemical ring-closing of the monomer.[22] However, neither the photochemical switching nor the photoluminescence of the switch were retained in the polymer films because of quenching due to H-aggregation of the sexithiophene units.[23] One approach that has been taken to prevent the loss of photochromic function upon electropolymerization is to introduce a spacer unit between the photoswitchable moiety and the unit responsible for electropolymerization.[24,25] Although this approach leads to polymer films that show reversible photochemical switching, the methoxystyryl units used to form the polymer through oxidative coupling resulted in poor photostability of the film overall, especially upon irradiation with UV light.[25]

In the present contribution, an alternative approach is taken to circumvent these complications by avoiding the use of a separate functional unit for electropolymerization. Here we take advantage of the oxidative dimerization of spiropyran **1** (*vide infra*; Scheme 1)[26,27] to form the polymer film and, simultaneously, the photochromic unit, i.e. the bis-spiropyran, thereby avoiding

the need to include a separate functional unit for polymerization. We show that the bis-spiropyran unit formed exhibits unprecedented redox- and $H^+$-gated photochromism (Scheme 2) and that these properties are retained after immobilization on conducting surfaces.

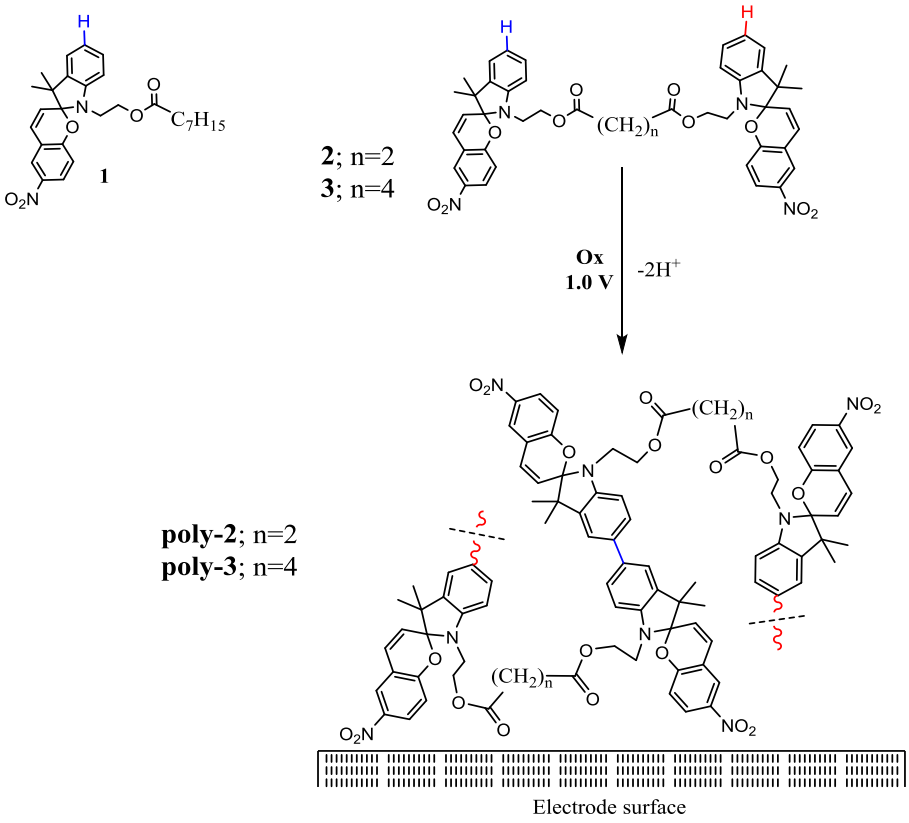


**Scheme 1.** Structures of spiropyran **1** and double (alkyl ester-bridged) spiropyrans **2** and **3**. Immobilization of **2** and **3** is achieved through sequential oxidative coupling of the indoline units.[28]

The photochromic properties of spiropyrans were first reported in 1952,[29] and they have been applied widely since in molecular-based devices.[30] The photochromism of spiropyrans is based on interconversion between the spiro (SP) and merocyanine (MC) forms (Scheme 2, top left). Upon irradiation with UV light, the spiropyran is converted to its merocyanine form, with reversion upon irradiation with visible light as well as thermally. Additionally, for a number of spiropyrans the photostationary state has been reported to shift in favor of the merocyanine form in the presence of a source of $H^+$.[31] The absorption spectrum of the protonated merocyanine is distinct from that of the nonprotonated merocyanine,[32] but nevertheless, irradiation with visible light regenerated the spiropyran form with rerelease of the $H^+$, a behavior that has indeed proven useful in exerting subtle control over pH.[33]

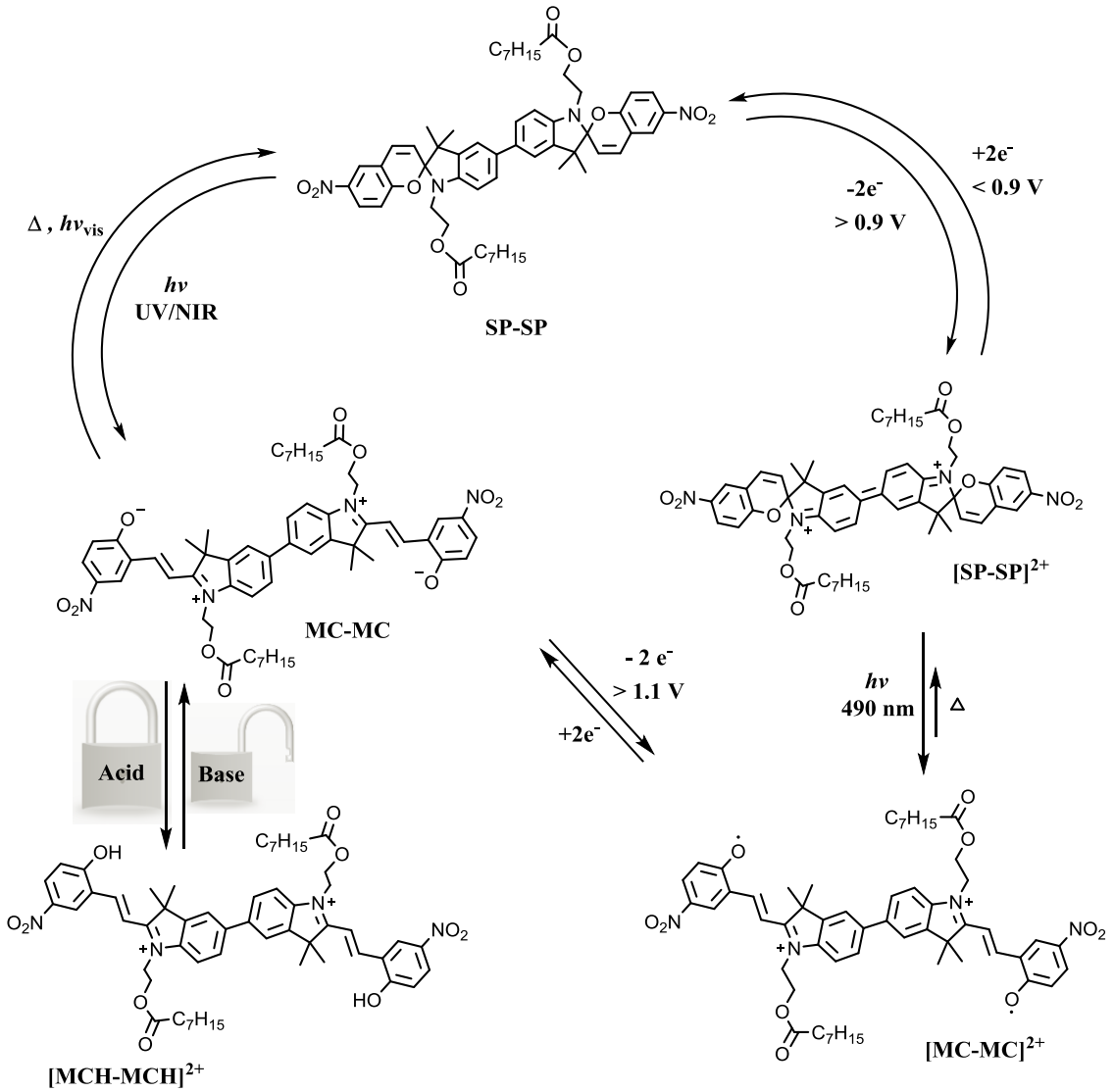


**Scheme 2.** pH- and redox-gated photochemical switching between the bis-spiropyran (**5**) and its bis-merocyanine form.

Although the redox chemistry of spiropyrans has been noted on several occasions, their potential use in electrochemical applications has focused primarily on the change in polarity induced by photochemical switching.[34,35,36] The first report of the redox chemistry of the spiropyran unit itself was by Campredon *et al*. in 1993.[37] However, the electrochemical mechanisms observed[38] were clarified only relatively recently when it was established that dimerization through the 5-position of the indoline unit of, e.g., 2-(3',3'-dimethyl-6-nitrospiro[chromene-2,2'-indolin]-1'-yl)ethyl octanoate (**1**) (Scheme 3) occurs.[27] Such dimerization was shown to be blocked effectively by the incorporation of a methyl group at that position (i.e., in **6**).[27] The dimerization of spiropyrans is manifested in their cyclic voltammetry by an irreversible oxidation at ca. 1.05 V vs SCE (Scheme 3), which results in coupling and subsequent double deprotonation. The bis-spiropyran formed is oxidized immediately to its dicationic state and subsequently undergoes stepwise reduction at *ca.* 0.8 and 0.65 V vs SCE. Overall its voltammetry resembles that of [3,3',5,5'-tetramethylbenzidine]$^{2+}$.[39] The fact that spiropyrans can undergo oxidative coupling in this way presents opportunities for the utilization of both their electro- and photochemistry[29,40] and raises questions regarding the photochemistry of the bis-spiropyran formed (Scheme 3).

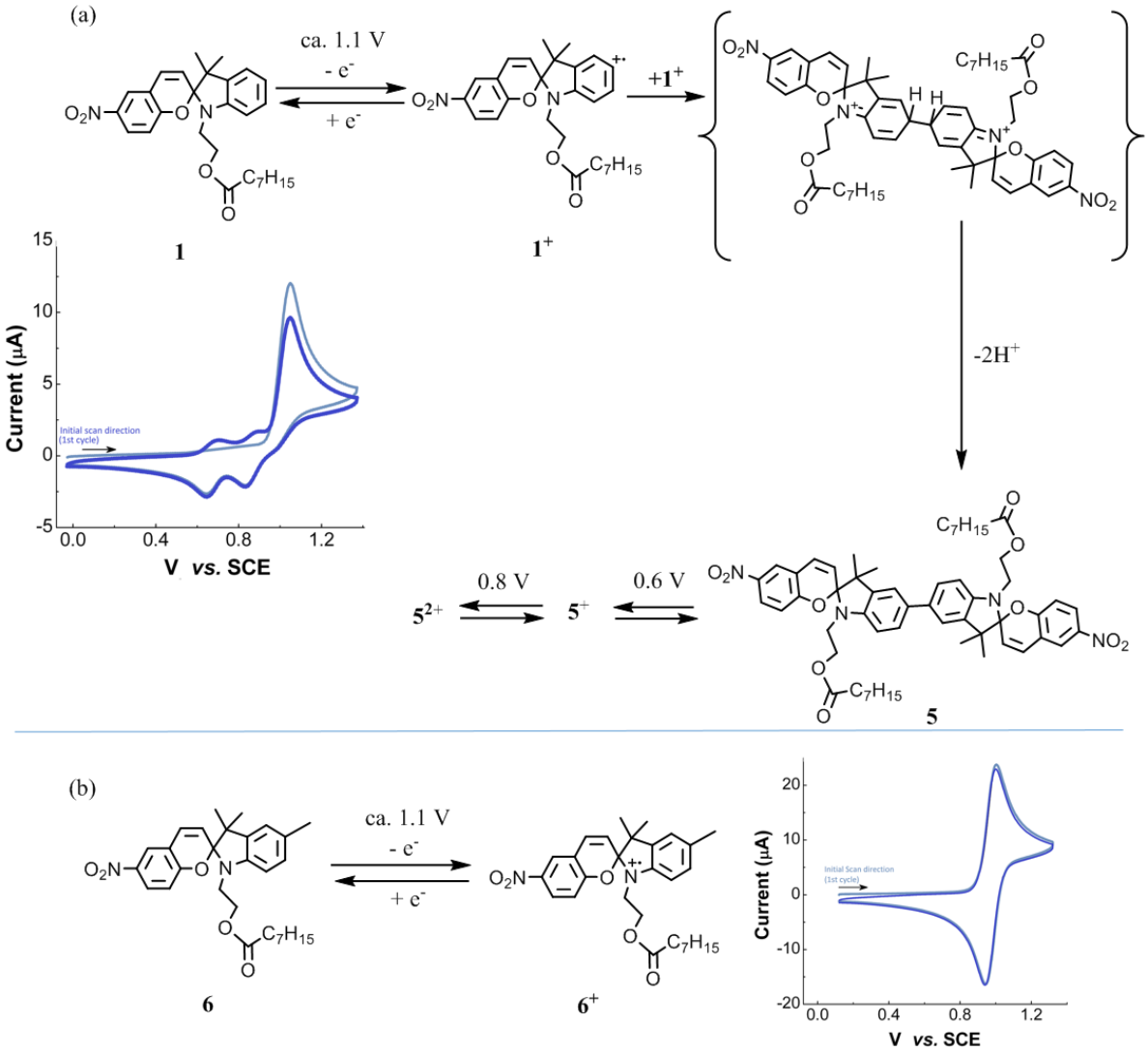


**Scheme 3.** (a) Mechanism for oxidative dimerization of **1** to form bis-spiropyran **5** and (inset) the corresponding cyclic voltammetry. (b) Reversible one-electron oxidation of **6**, for which the methyl group at the indoline 5-position prevents carbon-carbon bond formation. Data shown in insets are taken with permission from Ivashenko et al.[27]

In this work, we took advantage of the propensity of spiropyran **1** to undergo oxidative dimerization to form redox- and photoresponsive films through electropolymerization. Two spiropyrans were tethered covalently using bisester linkers of various lengths attached at the indoline nitrogen to form **2** and **3** (Scheme 1). Electrochemical coupling of two spiropyrans enabled the formation of polymers of alkyl diester-bridged bis-spiropyrans, in the case of **2** and **3**.

We show that although the already limited photochromic response of the bis-spiropyran (**5**) in solution is reduced further upon immobilization, the $H^+$-gated and electrochemically gated photochromic response is retained fully on the polymer-modified electrodes. Furthermore, immobilization as a thin film on an electrode allows for more rapid electrochemical/$H^+$-gated switching, with visible rather than UV light, than can be achieved in solution. Hence, rather than losing responsivity upon immobilization, as is often the case, the present system provides even more rapid access to the $H^+$-gated and electrochemically gated photochromism of **5**.

## Experimental Section

### Materials.

2-(3',3'-Dimethyl-6-nitrospiro[chromene-2,2'-indolin]-1'-yl)ethanol (**4**) was synthesized following literature procedures.[41] All of the chemicals for electrochemical measurements and for the synthesis of bis(2-(3',3'-dimethyl-6-nitrospiro[chromene-2,2'-indolin]-1'-yl)ethyl) succinate and bis(2-(3',3'-dimethyl-6-nitrospiro[chromene-2,2'-indolin]-1'-yl)ethyl) adipate were purchased from Aldrich or Acros and were used without further purification. Dichloromethane (DCM) was distilled over calcium hydride before use for chromatography, and spectroscopic-grade DCM (UVASOL) was used without additional purification for spectroscopic and electrochemical measurements.

### Synthesis of bis(2-(3',3'-dimethyl-6-nitrospiro[chromene-2,2'-indolin]-1'-yl)ethyl) succinate (2).

Compound **4** (0.58 g, 1.64 mmol), *N,N*-dimethylaminopyridine (DMAP) (0.20 g, 1.64 mmol), *N,N*-dicyclohexylcarbodiimide (DCC) (0.35 g, 1.7 mmol), and succinic acid (0.09 g, 0.82 mmol) were dissolved in DCM (50 mL) and stirred overnight at room temperature. The solution was washed with water (3 x 30 mL) and the organic layer was dried over $Na_2SO_4$. The solvent was removed in vacuo and the residue was purified by column chromatography over silica gel using pentane with an increasing gradient of ethyl acetate as the eluent, providing the product as a pink solid in 58% yield (0.75 g, 0.95 mmol). Mp: 81.0-83.5°C. $^1$H NMR ($CDCl_3$): δ 8.03 (d, J = 2.6 Hz, 2H), 7.98 (s, 2H), 7.19 (t, J = 7.7 Hz, 2H), 7.09 (d, J = 6.5 Hz, 2H), 6.91 (d, J = 9.7 Hz, 2H), 6.89 (t, J = 8.1 Hz, 2H), 6.74 (d, J = 9.7 Hz, 2H), 6.65 (d, J = 7.7 Hz, 2H), 4.32-4.14 (m, 4H), 3.60-3.28 (m, 4H), 2.51 (s, 4H), 1.27 (s, 6H), 1.15 (s, 6H). $^{13}$C NMR ($CDCl_3$): δ 172.1, 159.5, 146.7, 141.2, 135.8, 128.5, 128.0, 126.1, 122.9, 122.0, 121.9, 120.1, 118.6, 115.7, 106.8, 106.6, 62.9, 53.0, 42.5, 28.9, 26.0, 20.0. ESI-MS: m/z 787.2980 $[M+H]^+$; calcd for $C_{44}H_{43}N_4O_{10}$, 787.2974. Anal. Calcd for $C_{44}H_{42}N_4O_{10}$: C, 67.2; H, 5.38; N, 7.12. Found: C, 67.4; H, 5.48; N, 6.98.

### Synthesis of bis(2-(3',3'-dimethyl-6-nitrospiro[chromene-2,2'-indolin]-1'-yl)ethyl) adipate (3).

Compound **4** (1.00 g, 2.8 mmol), DMAP (0.34 g, 2.8 mmol), DCC (0.62 g, 3.0 mmol) and adipic acid (0.20 g, 1.4 mmol) were dissolved in DCM (50 mL) and stirred overnight at room temperature. The solution was washed with water (3 x 30 mL) and dried over $Na_2SO_4$. The solvent was removed *in vacuo*, and the residue was purified by column chromatography over silica gel using pentane with an increasing gradient of ethyl acetate as the eluent, providing the product as a pink solid in 65% yield (0.73 g, 0.91 mmol). Mp: 77.8-77.9°C. $^1$H NMR ($CDCl_3$): δ 8.02 (d, *J* = 2.6 *Hz*, 2H), 8.00 (s, 2H), 7.19 (t, *J* = 7.7 *Hz*, 2H), 7.08 (d, *J* = 7.1 *Hz*, 2H), 6.92 (d, *J* = 10.1 *Hz*, 2H), 6.89 (t, *J* = 7.7 *Hz*, 2H), 6.74 (d, *J* = 8.5 *Hz*, 2H), 6.67 (d, *J* = 7.8 *Hz*, 2H), 5.87 (d, *J* = 10.4 *Hz*, 2H), 4.31-4.11 (m, 4H), 3.55-3.34 (m, *J* = 21.4 *Hz*, 15.1 *Hz*, 6.3 *Hz*, 4H), 2.22 (bs, 4H), 1.55 (m, 4H), 1.28 (s, 6H), 1.16 (s, 6H). $^{13}$C NMR ($CDCl_3$): δ 173.1, 159.5, 146.8, 141.2, 135.8, 128.5, 128.0, 126.1, 122.9, 122.0, 121.9, 120.1, 118.6, 115.7, 106.8, 106.6, 62.6, 53.0, 42.5, 33.8, 26.0, 24.3, 20.0. ESI-MS: *m/z* 815.3419 $[M+H]^+$; calcd for $C_{46}H_{47}N_4O_{10}$: 815.3827. Anal. Calcd for $C_{46}H_{46}N_4O_{10}$: C, 67.8; H, 5.69; N, 6.88. Found: C, 67.6; H, 5.93; N, 6.68.

### Synthesis of 2-(3',3'-dimethyl-6-nitrospiro[chromene-2,2'-indolin]-1'-yl)ethyl octanoate (1).

Compound **4** (1.11 g, 3.0 mmol), octanoic acid (0.47 g, 3.3 mmol), *N*-(3-(dimethylamino)propyl)-*N'*-ethylcarboiimide hydrochloride (EDCI), (0.63 g, 3.3 mmol) and *N*-hydroxybenzotriazole (HOBt)

(0.42 g, 3.1 mmol) were dissolved in 40 mL of DCM, and the solution was stirred overnight under a nitrogen atmosphere. The organic layer was washed with aqueous $NaHCO_3$ (2 x 20 mL) and water (3 x 20 mL) and dried over $MgSO_4$. DCM was removed *in vacuo*. Purification of the crude product by column chromatography over silica gel using pentane with an increasing gradient of DCM as the eluent provided the product as a yellow solid in 23% yield (0.33 g, 0.69 mmol). $^1$H NMR ($CDCl_3$) δ 0.86 (m, J = 6.8 Hz, 3H), 1.14 (s, 3H), 1.17-1.30 (br, 8H), 1.27 (s, 3H), 1.53 (m, 2H), 2.22 (t, J = 6.8 Hz, 2H), 3.38 (m, 1H), 3.45 (m, 1H), 4.16 (m, 1H), 4.22 (m, 1H), 5.87 (d, J = 10.3 Hz, 1H), 6.66 (d, J = 8.4 Hz, 1H), 6.72 (d, J = 7.8 Hz, 1H), 6.87 (m, 2H), 7.06 (d, J = 7.3 Hz, 1H), 7.19 (t, J = 7.8 Hz, 1H), 7.98 (s, 1H), 8.00 (d, J = 7.3 Hz, 1H).

### Synthesis of 2-(3',3'-dimethyl-6-nitrospiro[chromene-2,2'-indolin]-1'-yl)ethyl octanoate dimer (5).

Compound **1** (0.20 g, 0.42 mmol) was dissolved in 20 mL of $CH_3CN$ and 163 mg of $Cu(ClO_4)_2 \cdot 6\ H_2O$ was dissolved in 400 µL of water. The aqueous solution containing $Cu(ClO_4)_2 \cdot 6\ H_2O$ was added to the organic solution, and the reaction mixture was stirred at room temperature for 24 h. The solvent was then evaporated under reduced pressure, and the crude material was dissolved in 40 mL of DCM and filtered. The filtrate was washed with a saturated solution of $NaHCO_3$ containing 5% EDTA (3 x 20 mL). The organic phase was then dried over $Na_2SO_4$ and the solvent was distilled *in vacuo* to afford a brown solid. Purification by preparative TLC (silica, 20 cm x 20 cm, 1500 µm) with 30% EtOAc/pentane as the eluent yielded, next to the starting material, the product in 34% yield (34 mg, 0.036 mmol). $^1$H NMR ($CDCl_3$): δ 0.85 (t, 3H), 1.10-1.40 (br, 13H), 1.57 (m, 3H), 2.24 (m, 2H), 3.47 (m, 2H), 4.24 (m, 2H), 5.91 (d, 1H), 6.73 (d, 1H), 6.78 (d, 1H), 6.93 (d, 1H), 7.24 (s, 1H), 7.33 (d, 1H), 8.01 (s, 1H), 8.06 (m, 1H).

### Physical Methods.

$^1$H and $^{13}$C NMR spectra were obtained on a Varian Mercury Plus 399.93 MHz spectrometer. Chemical shifts (δ) are reported in parts per million and coupling constants in hertz. Integrations are also reported, and multiplicities are denoted as follows: s = singlet, d = doublet, t = triplet, br = broad singlet, m = multiplet. Chemical shifts are reported with respect to tetramethylsilane and referenced to residual solvent ($CHCl_3$) signals. Mass spectra were recorded on a ThermoScientific LTQ Orbitrap XL spectrometer. UV/vis absorption spectra were obtained on an Analytik Jena Specord600 spectrometer. Electrochemical data were obtained using a 600C or 760B electrochemical workstation (CH Instruments). The working electrodes used were a Teflon-shrouded glassy carbon electrode (3 mm diameter), indium tin oxide (ITO) on glass slides (1 cm x 3 cm), a platinum disc electrode (2 mm diameter), and gold beads.[42] A platinum wire was used as an auxiliary electrode, and a Ag/AgCl reference electrode or a saturated calomel electrode (SCE) was used as the reference electrode. Cyclic voltammograms were obtained at a sweep rate of 100 mV $s^{-1}$ in anhydrous DCM containing 0.1 M tetrabutylammonium chloride with analyte concentrations of 0.5 to 2 mM unless stated otherwise. All potential values are quoted with respect to SCE. Redox potential ($E_{p,a}$, anodic peak potential; $E_{p,c}$, cathodic peak potential; $E_{½}$ = ($E_{p,a}$+$E_{p,c}$)/2) values are ±10 mV. UV/vis absorption spectroelectrochemistry of **5** was carried out using an optically transparent thin-layer electrochemical (OTTLE) cell (a liquid IR cell modified with Infrasil windows, platinum mesh working and counter electrodes and a Ag/AgCl reference electrode; University of Reading) mounted in a Specord600 UV/vis absorption spectrometer with the potential controlled by a CHI760B potentiostat. The Ag/AgCl reference electrode of the OTTLE

cell was prepared by anodization at 9 V with a platinum wire cathode in 3 M KCl(aq). In situ UV/vis absorption spectroelectrochemistry of poly-**2** and poly-**3** was carried out by initial modification of an ITO electrode by cyclic voltammetry followed by transfer to a quartz cuvette as an electrochemical cell. Irradiation at 365 nm (4.1 mW), 490 nm (2 mW), and 660 nm (4.5 mW) was provided by laser diodes (Thorlabs).

## Results and discussion

The syntheses and electrochemical and spectroscopic characterizations of compounds **4**,[41] **1** and **5**[26] (**Scheme 4**) were reported earlier. Although electrochemical dimerization of **1** was carried out previously,[27] for convenience oxidative dimerization of **1** was carried out with a Cu(II) salt using the method described by Natali and Giordani.[26] to yield spiropyran dimer **5** in 34% yield (**Scheme 4**). The spectroscopic properties of the obtained product (SOI, **Figure S1** and **S2**) were identical to those of the product previously obtained by electrochemical oxidative coupling.[26] Compounds **2** and **3** were prepared from **4** by reaction with succinic and adipic acid, respectively (**Scheme 4**).

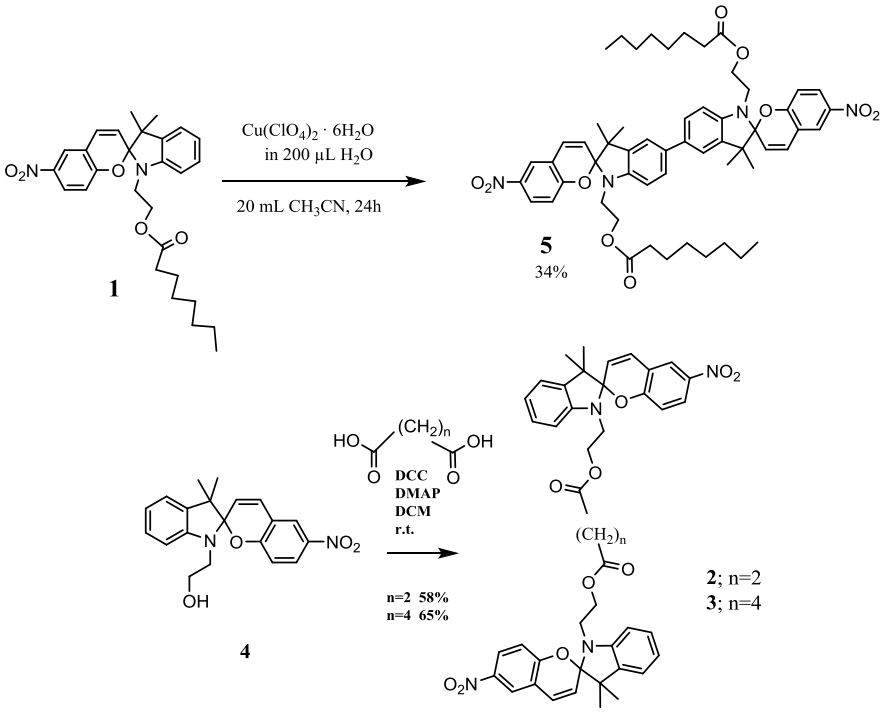


**Scheme 4.** Synthesis of **5** through chemical oxidative dimerization of **1** and synthesis of **2** and **3** from **4** through DCC coupling.

### *pH gated photochromism of 5*

Bis-spiropyran **5** shows absorption at < 400 nm, which upon irradiation at $\lambda_{exc}$ = 365 nm results in the appearance of a visible absorption band at 600 nm assigned to the merocyanine form (**Figure 1**). Thermal reversion is rapid once irradiation is ceased.[26] Addition of $CF_3SO_3H$ at the photostationary state at 365 nm results in an immediate blue shift of the visible absorption band to 507 nm, with a shoulder at 441 nm. Further irradiation at 365 nm results in a substantial increase in the absorbance of this new band (**Figure 1**). Subsequent irradiation at 490 nm had no effect on the absorption spectrum, confirming both the thermal and photochemical stability of the protonated merocyanine form of **5**. Addition of $Et_3N$, however, resulted in an immediate red shift in the visible absorption band from 507 to 600 nm followed by rapid thermally driven

recovery of the original absorption spectrum of the spiropyran form of **5** (Figure 2). The thermal stability of the bis-spiropyran form of **5** in the absence of acid was complete (i.e., the ring-opened form was not observed), indicating that the difference in ground-state energies of the two forms is high. Under acidic conditions, however, ring opening to form the merocyanine was observed over long periods (> 3 h), indicating that it is more stable than the spiropyran form, which is consistent with its more positive oxidation potential (*vide infra*), and that the barrier to thermal isomerization is controlled by the interchange between the spiro and deprotonated merocyanine forms.

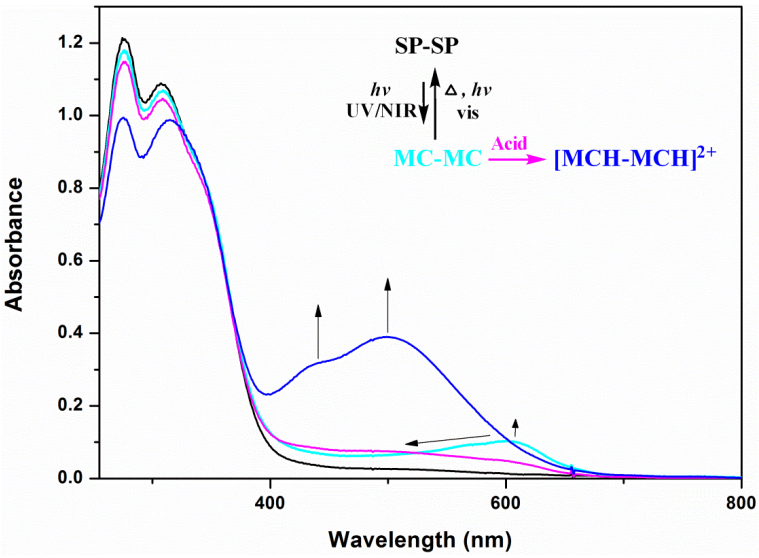


**Figure 1.** UV/vis absorption spectrum of **5** (1 mM in DCM containing 0.1 M $TBAPF_6$) before (black) and after (light blue) irradiation at $\lambda_{exc}$ = 365 nm. Addition of $CF_3SO_3H$ results in a blue shift in the absorption spectrum (pink), and subsequent irradiation at 365 nm yields the bis-merocyanine form of **5** (dark blue).

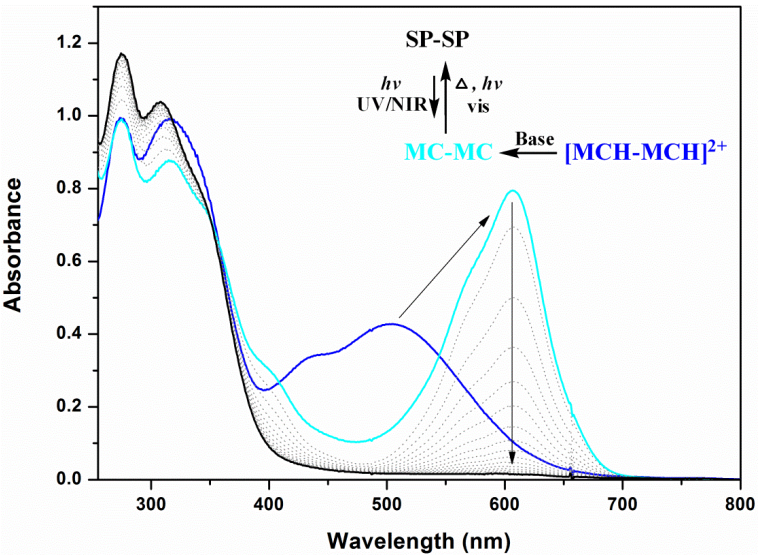


**Figure 2.** UV/vis absorption spectrum of the protonated bis-merocyanine form of **5** (dark blue) (1 mM in DCM containing 0.1 M $TBAF_6$) generated by irradiation at $\lambda_{exc}$ = 365 nm after addition of $CF_3SO_3H$ (dark blue). Subsequent addition of $Et_3N$ (light blue) is followed by thermal recovery (dotted lines recorded at 7.5 s intervals) of the spectrum of bis-spiropyran **5** (black line).

*UV/vis/NIR absorption spectroelectrochemistry of 5*

The cyclic voltammetry of **5** is characterized by two reversible oxidation waves at 0.65 and 0.80 V vs SCE (**Scheme 3**).[26] Electrochemical oxidation of **5** to its monocationic form $\mathbf{5}^{+}$ resulted in the appearance of bands at 445 and 470 nm together with near-IR (NIR) absorption bands at ca. 770, 870, and 995 nm, which are characteristic of a $TMB^{+}$-type radical cation (**Figure 3**).[43]

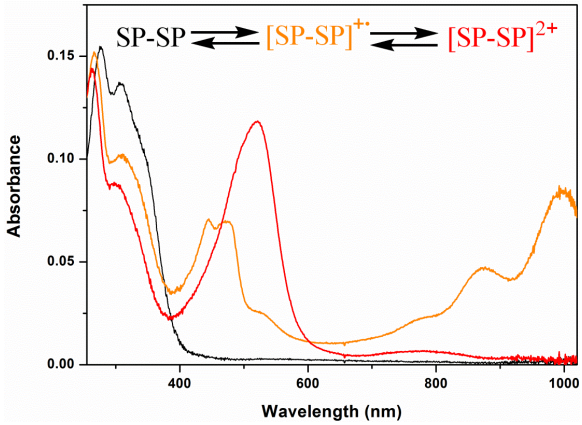


**Figure 3.** In situ UV/vis absorption spectra of **5** obtained during thin-layer cyclic voltammetry at 0.7 (orange) and 0.9 V (red).

Oxidation at more positive potentials resulted in a loss of the NIR absorption band and a red-shift and increase in visible absorption at 525 nm due to formation of dicationic $\mathbf{5}^{2+}$, as described previously.[27] The changes in the absorption spectrum of **5** were reversed fully upon application of a potential of < 0.6 V, confirming that the spiropyran structure is unaffected by oxidation. Notably, however, when UV/vis absorption spectra were acquired at short time intervals when **5** was in its oxidized state (i.e., $\mathbf{5}^{2+}$), the initial absorption spectrum did not recover fully. Instead, weak visible absorption bands remained after reduction at 0.0 V, indicating that $\mathbf{5}^{2+}$ is photochemically active. Indeed, when spectra were recorded continuously when the potential was held more positive than that of the second redox wave, the conversion to this second species was complete (**Figure 4**). Subsequent reduction at 0 V resulted in the disappearance of the band at 780 nm, confirming that the photochemical product is also redox-active, with a visible absorption band remaining at 430 nm that is both thermally and photochemically stable.

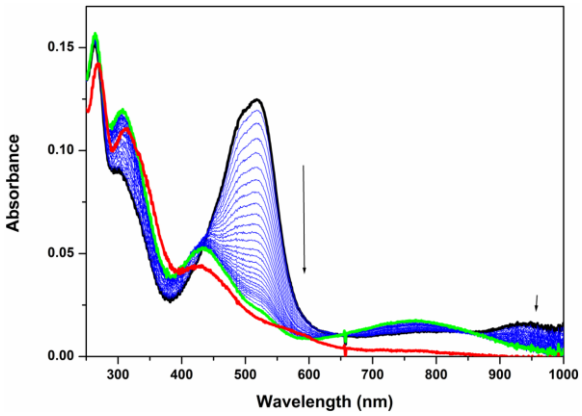


**Figure 4.** Changes in the UV/vis absorption spectrum of **5** (1 mM) oxidized at 1.1 V (thick black line) during sequential acquisitions (shown at 7 s intervals in blue; the final spectrum is shown in green) followed by reduction at 0.0 V (red).

Although irradiation of the neutral bis-spiropyran **5** at 365 nm results in the appearance of an absorption band at 600 nm and, in the presence of acid, a stronger absorption band at 507 nm, irradiation of **5** with visible light (e.g., 490 nm) has no effect on its absorption spectrum. Furthermore, neither the protonated merocyanine form (*vide supra*) nor the monocationic form $\mathbf{5}^{+}$, are affected by irradiation at 365 or 490 nm.

The dication $\mathbf{5}^{2+}$ is thermally stable, in contrast to related indolinooxazolidines.[44] Irradiation at 490 nm (i.e., in resonance with the absorption band of $\mathbf{5}^{2+}$ at 525 nm) results in a rapid decrease in absorbance at 525 nm and the appearance of broad visible absorption bands at 420 and 750 nm (**Figure 5**). When irradiation is ceased, the spectrum recovers partially, i.e., the absorption band of $\mathbf{5}^{2+}$ at 525 nm increases and the bands at 420 and 750 nm decrease again. Subsequent reduction at 0.0 V results in a loss of absorbance of $\mathbf{5}^{2+}$ and its primary photoproduct, but, the initial spectrum of **5** is not recovered fully (**Figure 5**). Instead, a broad absorption band is observed at 470 nm that is similar to the one observed upon protonation of the merocyanine form of **5** (**Figure 2**; *vide supra*). These data demonstrate for the first time that instead of suppressing the photochemistry of **5**, oxidation to the dicationic form enhances this photochemistry.

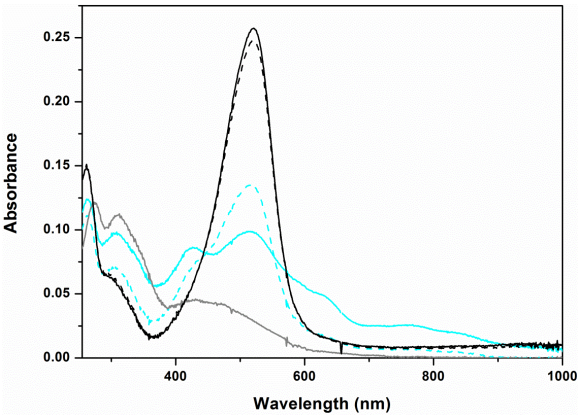


**Figure 5.** UV/vis absorption spectrum of $\mathbf{5}^{2+}$ (thick black line, generated by oxidation at 1.2 V) and spectra after 90 s at 1.2 V (dashed black line), after irradiation at 490 nm for 60 s (solid cyan line), and after 1 min without irradiation (dashed cyan line). The spectrum obtained after subsequent reduction at 0.0 V is shown as a solid gray line.

In summary, these data show that bis-spiropyran **5** is thermally stable in the neutral state and that UV irradiation converts it to its thermally unstable merocyanine form. Protonation of the merocyanine form renders it thermally and photochemically stable and allows the equilibrium position to be shifted in favor of the merocyanine form, as is observed frequently for monospiropyrans.[31,32,34] Hence, ring opening can be achieved by irradiation with UV light, and the ring-open state can then be "locked" by protonation and "unlocked" by deprotonation. In the dicationic state, $\mathbf{5}^{2+}$, ring opening to the merocyanine form proceeds smoothly using visible light, and although the oxidized merocyanine form is thermally unstable (reverting to the dicationic spiropyran form), it can be "locked" by protonation and subsequent reduction either during or after oxidation (*vide infra*). It should be noted that all steps (i.e., in **Scheme 2**) indicate that both spiropyran units undergo switching.[45] Intermediates in which switching of only one of the units has occurred are also possible. Indeed, this question is a central issue in the field of multiphotochromics.[46] In the present case of **5**, no evidence for such intermediate species is

available; this may be due to the increased aromatization of one indoline unit, which drives aromatization (and ring opening) of the second unit.

*Synthesis and characterization of 2 and 3*

As discussed above, immobilization of 5 as a polymer on electrodes was achieved by taking advantage of the propensity for spiropyrans to undergo oxidative dimerization (**Scheme 3**). The alkyl group on the indoline nitrogen is a key structural feature of the spiropyrans, as it provides an excellent platform for other functional units to be attached in a modular manner, allowing more complex responsive molecular systems to be synthesized. Two spiropyran units were tethered via a diester linker by esterification of **4** with succinic acid or adipic acid. The spectroscopic characterizations of compounds **2** and **3** are provided in the Experimental Section and Supporting Information. As stated above, a key question raised in the preparation of modified surfaces based on molecular switches, concerns the retention of functionality of the switchable unit after immobilization. Here, the bis-spiropyran was immobilized through electrochemical polymerization on ITO, glassy carbon, and Pt, and the effect of immobilization on the functional properties of the bis-spiropyran was examined using a combination of cyclic voltammetry, UV/vis/NIR absorption spectroscopy, and spectroelectrochemistry.

The cyclic voltammetry of **2** and **3** in the range of 0 to 1.2 V (**Figure 6**) is, as expected, very similar to that of monospiropyran **1**, with an oxidation peak at *ca.* 1.0 V assigned to oxidation of the indoline units, which is irreversible due to rapid dimerization (**Scheme 3**). In contrast to **1**, however, the oligomers formed deposit directly on the electrode resulting in an increase in current for the redox waves assigned to *poly*-**2**/*poly*-**2**$^{+}$ and *poly*-**2**$^{+}$/*poly*-**2**$^{2+}$ at 0.65 and 0.80 V, respectively, i.e., each of the spiropyran units in **2** and **3** undergoes a one-electron oxidation, after which coupling with another spiropyran radical occurs in an overall four-electron *ECCE* process (see **Scheme 3**), as observed previously for 2-(3',3'-dimethyl-6-nitrospiro[chromene-2,2'-indolin]-1'-yl)ethyl octanoate.[27]

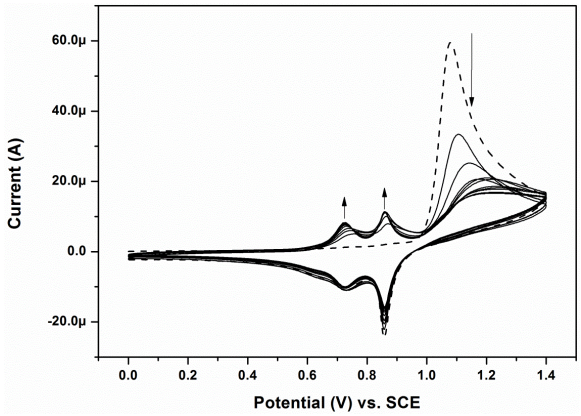


**Figure 6.** Cyclic voltammetry of **3** (1 mM in acetonitrile containing 0.1 M $TBAPF_6$) at a glassy carbon electrode (d = 3 mm) with a Pt counter electrode and an SCE working electrode at 0.1 V $s^{-1}$. The corresponding voltammetry at an ITO-on-glass electrode is shown in **Figure S3** (SOI).

The current response at > 1.05 V decreased over multiple cycles along with an increase in current response of the redox waves at 0.65 and 0.80 V, consistent with a buildup of poly-**2**/**3** at the electrode (**Figure 6**).[47] The decrease in current response at > 1.0 V is in part due to depletion of the diffusion layer, but stirring between cycles to "refresh" the depleted diffusion layer resulted in

only a slight recovery of its current response. This indicates that film formation results in a reduction, albeit a modest one, in the conductivity at the onset potential for oxidation of **2**/**3** although the film continues to grow in thickness with each cycle. Polymer film formation was also observed in acetonitrile or 1,2-dichloroethane, as well as on platinum, gold, and ITO electrodes. The formation of thicker films was observed on ITO electrodes compared with glassy carbon electrodes, which is ascribed to the former's increased roughness, and films of sufficient thickness for UV/vis/NIR absorption spectroscopy studies were obtained readily (**Figure 8**; *vide infra*).

*Cyclic voltammetry at poly-2 and poly-3 modified electrodes*

For both polymers, two fully reversible oxidation waves at 0.65 V and 0.80 V (**Figure 7**) are observed in monomer-free solution. The cyclic voltammetry at the electrodes modified with spiropyrans poly-**2** and poly-**3** shows a linear dependence on the scan rate, and for both, $E_{p,a} = E_{p,c}$ and $I_{p,a} = I_{p,c}$ for both redox waves, as expected for surface-confined redox processes. Continuous repeated cyclic voltammetry at 0.1 V $s^{-1}$ results in only a slight decrease in $I_{p,a}$ due primarily to peak broadening indicating both good adhesion of the film to the glassy carbon electrode and stability of the film in all three oxidation states. The non-Faradaic current shows a linear dependence on the scan rate (capacitance = 50 ± 1 µF $cm^{-2}$) and is unaltered by repeated cyclic voltammetry, further indicating that the film is not altered significantly upon oxidation and reduction (**Figure 7**). The absence of a significant redox wave at 1.1 V on poly-**2**/**3**-modified electrodes indicates that the degree of polymerization is high, as the polymer chain ends (i.e., nondimerized spiropyran units) would be expected to show a reversible redox wave at a potential similar to that of **6** (**Scheme 3**) due to entrapment of monospiropyran moieties within the polymer film with no opportunity to dimerize.

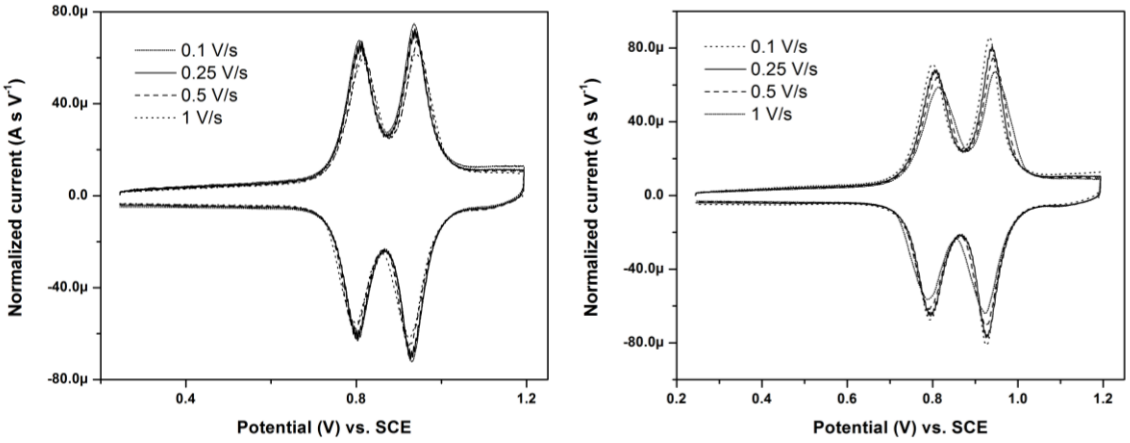


**Figure 7.** Scan-rate dependence of (electrochemically) deposited (left) *poly*-**2** and (right) *poly*-**3** on a glassy carbon working electrode (3 mm diameter) in monomer-free solution with the current normalized to the scan rate. The surface coverage estimated by integration was 7.3 ×$10^{-10}$ mol $cm^{-2}$, which corresponds to between 1 and 2 densely packed monolayer equivalents.

A key feature of redox polymers is that charge transfer from the electrode can be blocked except at potentials close to the formal potentials of the redox processes. This phenomenon is especially apparent as the polymer formed increases in thickness, i.e., as it forms a blocking layer at the electrode. The poly-**2** and poly-**3** films formed were probed for their ability to passivate the electrode at high redox potentials using the cationic redox probe[48] $[Ru(ph_2phen)_3]PF_6$ (where $ph_2phen$ = 1,10-diphenylphenanthroline), which is oxidized at 1.3 V vs SCE.[27,49] The

electrochemical response of a poly-**3** modified glassy carbon working electrode in monomer free solution showed the expected two reversible redox waves at 0.65 V and 0.80 V (SOI, **Figure S4**). Addition of $[Ru(ph_2phen)_3]PF_6$ had essentially no effect on the voltammetry at the electrode between 0.0 and 1.4 V vs SCE, confirming that redox conductivity of the fully oxidized polymer was absent (i.e., that electron transfer to and from the electrode was blocked effectively at potentials less and more positive than those of spiropyran polymer) and that coverage of the electrode surface by the polymer was complete. Continuous cyclic voltammetry, however, showed a steady increase in current response from $[Ru(ph_2phen)_3]PF_6$ over time concomitant with a decrease in the current response of poly-**3** (SOI, **Figure S4**). This change in response with cycling was not observed in the absence of $[Ru(ph_2phen)_3]PF_6$. Notably, the capacitance (i.e., non-Faradaic current) of the electrode was unaffected over the entire period indicating that the change in redox response was not due to desorption of the film. Furthermore, when the electrode was subsequently washed with solvent and transferred to a solution containing only electrolyte, the redox response of $[Ru(ph_2phen)_3]PF_{6\ 2}$ was no longer observed, confirming that it was not absorbed into the film. The redox waves of the spiropyran polymer did not show further changes even after standing in solution for 24 h. Returning the electrode to a 1 mM solution of $[Ru(ph_2phen)_3]PF_6$ showed an almost identical response as obtained 24 h previously (i.e., partial blocking of its current response), and continued cycling resulted in a further increase in conductivity at high potentials.

### *Vis/NIR absorption spectroelectrochemistry of poly-2 and poly-3*

Vis-NIR absorption spectroelectrochemistry of *poly*-**2**/**3** modified ITO electrodes showed the formation of the mono- and dicationic bis-spiropyrans (**Figure 8**), as observed for **5** in solution (*vide supra*).[50] Electrochemical oxidation of *poly*-**3** at 0.8 V to form *poly*-**3**$^+$ resulted in the appearance of absorption bands at 440 and 1000 nm. Subsequent oxidation at 0.9 V resulted in the disappearance of the NIR absorption band at 1000 nm and the appearance of a more intense visible band at 530 nm. The absorption spectra of each state are essentially the same as observed for *N,N*-dimethylaniline,[51] which represents the bis-indoline unit in bis-spiropyrans, and **5**.

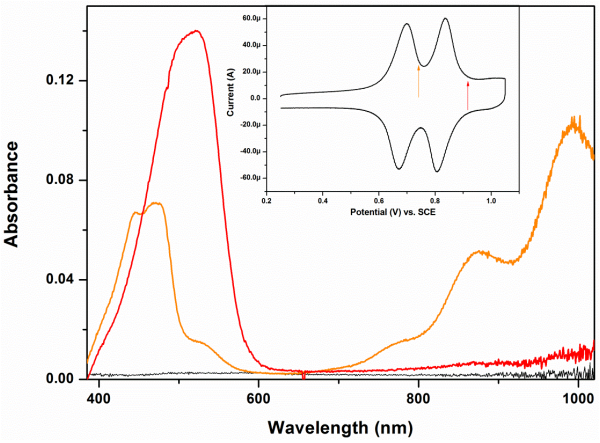


**Figure 8.** Vis/NIR absorption spectroelectrochemistry and (inset) cyclic voltammetry of a *poly*-**3** film on an ITO slide (in DCM containing 0.1 M $TBAPF_6$). Shown are the initial absorbance (black) and absorption spectra recorded during the cyclic voltammetry at the potentials indicated by the orange and red arrows in the inset.

### *Photochromism of poly-2 and poly-3*

The photochromism of *poly*-**2** and *poly*-**3** was established by both UV/vis absorption spectroscopy and cyclic voltammetry at ITO and glassy carbon electrodes. Irradiation of the as-formed polymer films did not result in a significant increase in visible absorption. As in the case of **5**, addition of acid (i.e., dilute $CF_3SO_3H$) resulted in switching-on of the photochromism of the polymer films upon irradiation at 365 nm, causing a rapid increase in visible absorption (**Figure 9**) identical to that observed for **5** in solution (**Figure 3**).

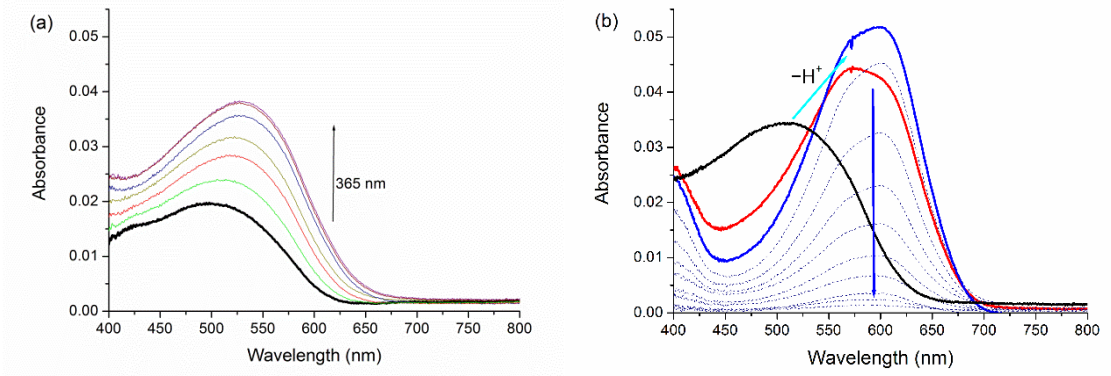


**Figure 9.** UV/vis absorption spectroscopy of a *poly*-**3**-modified ITO electrode in DCM with $CF_3SO_3H$ (1 mM) (a) after irradiation at 365 nm showing an increase in absorption at 525 nm, and (b) after irradiation at 365 nm (solid black line) followed by addition of $Et_3N$ (to 5 mM, red and blue lines; the blue arrow shows the direction of change in the spectrum), showing the decrease in visible absorption observed over time (thin lines, at 20 s intervals).

### *UV/vis absorption spectroelectrochemistry of photoswitched poly-3$^{2+}$*

The changes to the UV/vis/NIR absorption spectrum of a *poly*-**3** modified electrode upon oxidation at 0.65 and 0.80 V (**Figure 8**) are essentially identical to those observed for **5** (*vide supra*), with the appearance of absorption bands at 470 and ca. 1000 nm at 0.7 V, which are replaced at 0.9 V by a strong absorption at 525 nm (**Figure 10**). The band at 525 nm is stable at 0.9 V over time, but irradiation of the electrode at 490 nm at this potential resulted in a decrease in the absorption at 525 nm to leave a band at 500 nm. This band was unaffected by subsequent reduction at 0.0 V as at 1.0 V the photoproduct is immediately reduced (*vide infra*). Subsequent oxidation at 1.2 V resulted in an increase in absorbance at 430, 630, and 770 nm, corresponding to the oxidized protonated merocyanine form of **5**.

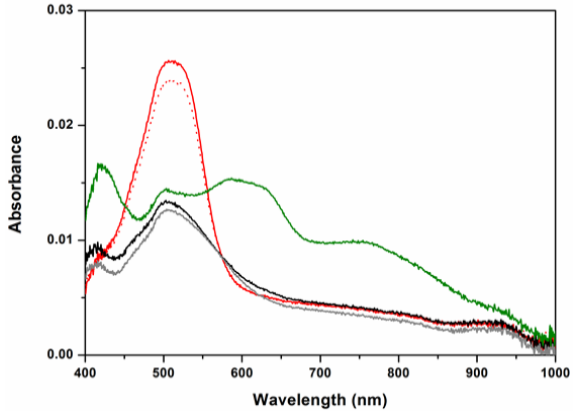


**Figure 10.** In situ UV/vis absorption spectroscopy of a *poly*-**3**-modified ITO electrode upon application of a potential of 0.9 V (red line) and after 30 s at 0.9 V(dotted red line). Irradiation at 490 nm for 15 s results in a decrease in visible absorbance (black line), which is unaffected by reduction at 0.0 V (gray lines). The spectrum after subsequent oxidation at 1.2 V is also shown (green line).

### *Electrochemically gated switching of poly-2 and poly-3*

Although *poly*-**2-** and *poly*-**3**-modified electrodes are stable over repeated cycling between 0.0 and 1.4 V vs SCE (*vide supra*), irradiation with visible light (i.e., at 490 nm) results in a decrease in the current of the two redox waves of the bis-spiropyran units and an increase in a redox wave at 1.2 V vs SCE (**Figure 11**).

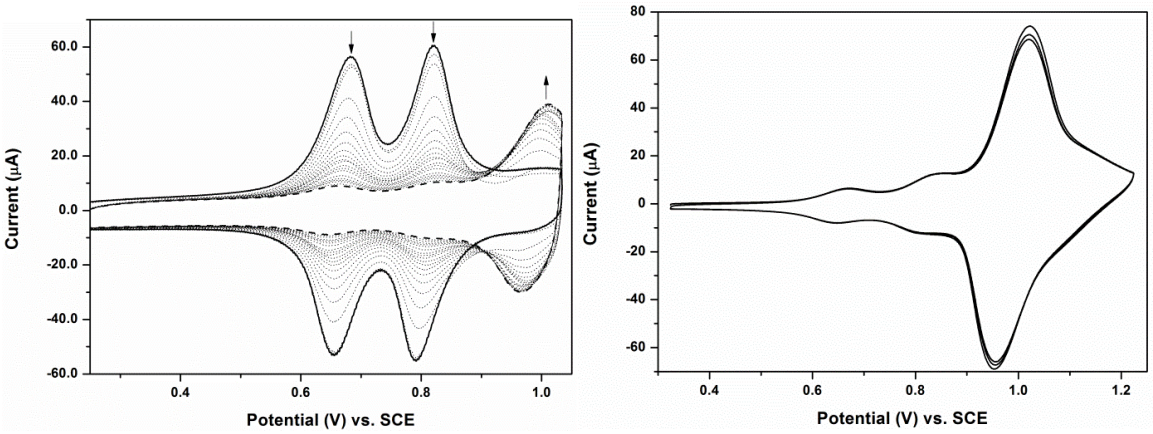


**Figure 11.** Cyclic voltammetry of a *poly*-**3**-modified ITO slide (DCM containing 0.1 M $TBAPF_6$, 0.1 V $s^{-1}$) (left) showing the effect of continuous irradiation at $\lambda_{exc}$ = 490 nm (2 mW $cm^{-2}$) during multiple cycles between 0.24 and 1.05 V vs SCE and (right) after irradiation is ceased.

Oxidation to the dicationic state poly-$\mathbf{3}^{2+}$ is required in order for photoconversion to be observed and the rate of switching at a glassy carbon electrode was found to be on the order of only < 15 s (SOI, **Figure S6**). Polarization of the electrode to 1.0 V is sufficient to oxidize poly-**3** to poly-$\mathbf{3}^{2+}$, but this potential is not sufficiently positive to oxidize the photoproduct, and hence, immediately after photochemical switching the product is reduced. This process is apparent from the charge passed at the working electrode, which initially is anodic (oxidation of poly-**3**) and upon commencement of irradiation becomes cathodic; ultimately the net charge passed is zero, confirming complete reduction of the film.

## Summary and Conclusions

Smart surfaces, i.e., surfaces that respond to combinations of orthogonal stimuli such as light, heat, pH etc., are highly desirable for a wide range of applications. Such surfaces require the use of components, typically molecular, that can achieve specific functions, and hence, a multimodal response requires the combination of multiple functional units. The use of molecular components that can carry out multiple distinct functions are therefore invaluable in reducing the synthetic complexity of smart surfaces. Furthermore, such units reduce the risk of undesirable cross-talk between components, such as quenching of photochemical activity. The preparation of photoswitchable polymers in principle requires the use of distinct units in their precursors, i.e., the photochromic unit itself and a unit that enables formation of the polymer. The properties of these units both before and after polymerization must be orthogonal in order to preserve the dual functionality of the system as a whole. The immobilization of polymers on conducting surfaces through electropolymerization is a highly attractive approach but brings with it challenges in regard to cross-talk between the functional units.

In this contribution, we have shown that bis-spiropyran **5** exhibits pH- and redox-gated photochromism. The opening of the spiro moieties to their merocyanine forms occurs upon irradiation with UV light, and they revert thermally and upon irradiation with visible light. Oxidation of **5** to $\mathbf{5}^{2+}$ results in a shift in its absorption spectrum to 520 nm, and remarkably, irradiation with visible light leads to conversion to the bis-merocyanine form. The conversion can be "locked" reversibly by protonation and reduction. These properties make **5** highly attractive as a component in responsive surfaces. The synthetic approach used to prepare bis-spiropyran **5** offers a distinct opportunity for polymerization to form poly-**2** and poly-**3** through combining the formation of the photochrome and the polymer in a single step. This combination is achieved by making the oxidative coupling of the two spiropyran units the final step in the formation of the polymer also and was achieved by tethering two spiropyran units via an alkyl chain in a manner that prevents intramolecular radical-radical coupling upon oxidation. This approach is made possible by the relative coincidence of the potential of the $\mathbf{5}^{+}/\mathbf{5}^{2+}$ redox couple and the onset potential for polymerization of the monospiropyran precursors **2** and **3**. Because the use of a separate polymerizable unit is avoided, the obtained polymer-modified electrodes retain the properties of **5**, and indeed, surface confinement on an electrode enables enhanced switching rates compared with those obtainable in solution.

This approach opens up new opportunities in creating multiresponsive surfaces, particularly in the dynamic control of electron transfer at interfaces and in the reversible switching of surface properties with visible light alone. The ability to control electron transfer at the electrode interface over a relatively wide, and physiologically relevant potential range opens up possibilities in the selective control of interfacial redox processes. Importantly, the present system allows switching between states to be achieved without the use of UV light, which is of particular benefit in terms of the stability of modified electrodes in operation. In a broader sense, the versatility of the present system in terms of switching possibilities opens up new prospects in applications in molecular logic,[52] with a single system providing an unprecedented degree of complexity in switching operation possible with a direct interface to the macroscopic world and hence high switching rates.

*The supporting information can be found online at DOI: 10.1021/jacs.5b11604*

## References

1 (a) Yerushalmi, R.; Scherz, A.; van der Boom, M. E.; Kraatz, H-B. *J. Mater. Chem*. **2005**, 15, 4480–4487; (b) Katsonis, N.; Lubomska, M.; Pollard, M. M.; Feringa, B. L.; Rudolf, P. *Prog. Surf. Sci.* **2007**, 82, 407–434; (c) Raymo, F. M.; Giordani, S.; White, A. J. P.; Williams, D. J. *J. Org. Chem.* **2003**, *68*, 4158-4169.

2 Wang, S.; Song, Y.; Jiang, L. *J. Photochem. Photobiol., C* **2007**, *8*, 18–29.

3 (a) Okano, T.; Yamada, N.; Okuhara, M.; Sakai, H.; Sakurai, Y. *Biomaterials* **1995**, 16, 297–303. (b) Khongtong, S.; Ferguson, G. S. *J. Am. Chem. Soc.* **2002**, *124*, 7254–7255.

4 Klein, J.; Kumacheva, E.; Mahalu, D.; Perahia, D.; Fetters, L. J. *Nature* **1994**, *370*, 634–636.

5 Galaev, I. Y.; Warrol, C.; Mattiasson, B. *J. Chromatogr. A* **1994**, *684*, 37–43.

6 Willner, I.; Basnar, B.; Willner, B. *Adv. Funct. Mater.* **2007**, *17*, 702-717.

7 Alexander, C.; Shakesheff, K. M. *Adv. Mater.* **2006**, *18*, 3321-3328.

8 Nogueira, A. F.; Toma, S. H.; Vidotti, M.; Formiga, A. L. B.;Córdoba de Torresi, S. I.; Toma, H. E. *New. J. Chem.* **2005**, *29*, 320-324.

9 Tomasulo, M.; Deniz, E.; Alvarado, R. J.; Raymo, F. M. *J. Phys. Chem. C* **2008**, 112, 8038–8045.

10 (a) Willner, I.; Willner, B. *J. Mater. Chem.* **1998**, *8*, 2543–2556. (b) Hauch, A.; Georg, A.; Baumgärtner, S.; Opara Krasovec, U.; Orel, B. *Electrochim. Acta* **2001**, *46*, 2131–2136.

11 Robertus, J.; Browne, W. R.; Feringa, B. L. Chem Soc. Rev. **2010**, *39*, 354-378.

12 (a) Katz, E.; Minko, S.; Halámek, J.; MacVittie, K.; Yancey, K. *Anal. Bioanal. Chem*. **2013** *405*, 3659-3672; (b) Doron, A.; Katz, E.; Tao, G.; Willner, I. *Langmuir* **1997**, *13*, 1783-1790.

13 (a) Leclerc, M. *Adv. Mater.* **1999**, *11*, 1491–1498. (b) Liu, Y.; Mu, L.; Liu, B. H.; Kong, J. L. *Chem.- Eur. J.* **2005**, *11*, 2622–2631.

14 Tomlinson, M. R.; Genzer, J. *Macromolecules* **2003**, *36*, 3449–3451.

15 (a) London, G.; Carroll, G. T.; Fernández Landaluce, T.; Pollard, M. M.; Rudolf, P.; Feringa, B. L. *Chem. Commun.* **2009**, 1712–1714; (b) Ivashenko, O.; Logtenberg, H.; Areephong, J.; Coleman, A. C.; Wesenhagen, P. V.; Geertsema, E. M.; Heureux, N.; Feringa, B. L.; Rudolf, P.; Browne, W. R. *J. Phys. Chem. C* **2011**, *115*, 22965–22975; (c) Doron, A.; Katz, E.; Tao, G.; Willner, I. *Langmuir* **1997**, *13*, 1783-1790.

16 (a) Ionov, L.; Sidorenko, A.; Stamm, M.; Minko, S.; Zdyrko, B.; Klep, V.; Luzinov, I. *Macromolecules* **2004**, 37, 7421–7423. (b) Fuhrmann, I.; Karger-Kocsis, J. *J. Appl. Polym. Sci.* **2003**, *89*, 1622–1630.

17 Kai, T.; Ueno, W.; Yamaguchi, T.; Nakao, S. *J. Polym. Sci., Part A: Polym. Chem.* **2005**, *43*, 2068–2074.

18 Browne, W. R. *Coord. Chem. Rev*. **2008**, *252*, 2470-2479.

19 Wolf, M. O.; Fox, M. A. *Langmuir* **1996**, *12*, 955-962.

20 Logtenberg, H.; Browne, W. R. *Org. Biomol. Chem.* **2013**, *11*, 233.

21 Tomasulo, M.; Yildiz, I.; Raymo, F. M. *Aust. J. Chem.* **2006**, *59*, 175-178.

22 (a) Areephong, J.; Kudernac, T.; de Jong, J. J. D.; Carroll, G. T.; Pantorott, D.; Hjelm, J.; Browne, W. R.; Feringa, B. L. *J. Am. Chem. Soc.* **2008**, *130*, 12850–12851; (b) Areephong, J.; Hurenkamp, J. H.; Milder, M. T. W.; Meetsma, A.; Herek, J. L.;Browne, W. R.; Feringa, B. L. *Org. Lett.* **2009**, *11*, 721-724.

23 Milder, M. T.; Herek, J. L.; Areephong, J.; Feringa, B. L.; Browne, W. R. *J. Phys. Chem. A.* **2009**, *113*, 7717-7724.

24 Logtenberg, H.; Jellema, L-J. C.; Lopez-Martinez, M. J.; Areephong, J.; Verpoorte, E.;

Feringa, B. L.; Browne, W. R. *Anal. Methods* 2012, *4*, 73−79.

25 Wesenhagen, P.; Areephong, J.; Fernandez Landaluce, T.; Heureux, N.; Katsonis, N.; Hjelm, J.; Rudolf, P.; Browne, W. R.; Feringa, B. L., *Langmuir* 2008, *24,* 6334-6342.

26 Natali, M.; Giordani, S., *Org. Biomol. Chem.* 2012, *10*, 1162-1171.

27 Ivashenko, O.; van Herpt, J. T.; Rudolf, P.; Feringa, B. L.; Browne, W. R. *Chem. Commun*. 2013, *49*, 6737-6739.

28 The oxidative coupling of the spiropyrans results in the release of two protons, however, the spiropyran itself remains in the spiro state and hence is unable to accept the protons released. The protons are instead scavenged effectively by adventitious proton acceptors (e.g., water) in the solvent, which is a subsequent source of protons for protonation of the merocyanine form upon ring opening.

29 Fischer, E.; Hirshberg, Y. *J. Chem. Soc.* 1952, 4522-4524.

30 *Molecular Switches*, 2nd ed.; Feringa, B. L., Browne, W. R., Eds.; Wiley VCH: Weinheim, Germany, 2011; Vols. 1 and 2.

31 (a) Maity, C.; Hendriksen, W. E.; van Esch, J. H.; Eelkema, R. *Angew. Chem. Int. Ed*. 2015, 54, 998–1001. (b) Giordani, S.; Cejas, M. A.; Raymo, F. M. *Tetrahedron* 2004, 60, 10973–10981. (c) Sumaru, K.; Kameda, M.; Kanamori, T.; Shinbo, T. *Macromolecules* 2004, *37*, 4949-4955. (d) Angiolini, L.; Benelli, T.; Giorgini, L.; Raymo, F. M., *Macromol. Chem. Phys*. 2008, 209, 2049–2060. (e) Silvi, S.; Arduini, A.; Pochini, A.; Secchi, A.; Tomasulo, M.; Raymo, F. M.; Baroncini, M.; Credi, A. *J. Am. Chem. Soc*. 2007, 29, 13378-13379.

32 (a) Raymo, F. M.; Giordani, S.; White, A. J.; Williams, D. J. *J. Org. Chem*. 2003, 68, 4158-4169. (b) Angiolini, L.; Benelli, T.; Bicciocchi, E., Giorgini, L.; Raymo, F. M. *React. Funct. Polym.* 2012, 72, 7, 469–477.

33 Silvi, S.; Constable, E. C.; Housecroft, C. E.; Beves, J. E.; Dunphy, E. L.; Tomasulo, M.; Raymo, F. M.; Credi, A. *Chem. Commun*. 2009, 1484–1486.

34 (a) Doron, A.; Katz, E.; Tao, G.; Willner, I. *Langmuir* 1997, *13*, 1783-1790. (b) Katz, E.; Willner, I. *Electroanalysis* 1995, *7*, 417-419.

35 Perrier, A.; Maurel, F.; Jacquemin, D. *Acc. Chem. Res.* 2012, *45*, 1173–1182.

36 Ivashenko, O.; van Herpt, J. T.; Feringa, B. L.; Rudolf, P.; Browne, W. R. *J. Phys. Chem. C* 2013, *117*, 18567-18577.

37 Campredon, M.; Giusti, G.; Guglielmetti, R.; Samat, A.; Gronchi, G.; Alberti, A.; Benaglia, M. *J. Chem. Soc., Perkin Trans. 2* 1993, 2089-2094.

38 (a) Preigh, M. J.; Stauffer, M. T.; Lin, F.-T.; Weber, S. G. *J. Chem. Soc. Faraday Trans.* 1996, *92*, 3991-3996. (b) Zhi, J. F.; Baba, R.; Hashimoto, K.; Fujishima, A. *J. Photochem. Photobiol., A* 1995, *92*, 91-97. (c) Doménech, A.; García, H.; Casades, I.; Esplá, M. *J. Phys. Chem. B* 2004, 108, 20064-20075. (d) Wagner, K.; Byrne, R.; Zanoni, M.; Gambhir, S.; Dennany, L.; Breukers, R.; Higgins, M.; Wagner, P.; Diamond, D.; Wallace, G. G.; Officer, D. L. *J. Am. Chem. Soc.* 2011, *133*, 5453-5462.

39 Owano, H.; Murakami, H.; Yamashita, T.; Ohigashi, H.; Ogata, T. *Synth. Met.* 1991, *39*, 327-341.

40 Guragain, S.; Bastakoti, B. P.; Ito, M.; Yusa, S.; Nakashima, K. *Soft Matter* 2012, *8*, 9628-9634.

41 Lee, S. J.; Jung, S. H.; Lee, S.; Han, W. S.; Jung J. H. *J. Nanosci. Nanotechnol*. 2009, *9*, 5990-5996.

42 Browne, W. R.; Kudernac, T.; Katsonis, N.; Areephong, J.; Hjelm, J.; Feringa, B. L. *J. Phys. Chem. C* 2008, *112*, 1183−1190.

43 (a) Hasegawa, H. *J. Phys. Chem*. 1961, *65*, 292-296 (b) Kiruthiga, K.; Aravindan, P.; Anandan, S.; Maruthamuthu, P. *Res. Chem. Intermed.* 2006, *32*, 115-135.

44 Szalóki, G.; Alévêque, O.; Pozzo, J.-L.; Hadji, R.; Levillain, E.; Sanguinet, L. *J. Phys. Chem. B* 2015, *119*, 307–315.

45 A further issue is the extent of protonation. In the present study, excess acid and base were used to ensure that only fully protonated or fully deprotonated states were reached.

46 Fihey, A.; Perrier, A.; Browne, W. R.; Jacquemin, D. *Chem. Soc. Rev*. 2015, *44*, 3719-3759.

47 The proximity of the indoline units could result in intramolecular coupling, especially at low concentration. However, space filling models of spiropyrans **2** and **3** indicate that the strain would preclude intramolecular coupling to a significant extent. In addition, the formation of macrocycles is entropically unfavorable.

48 Kapturkiewicz, A. *Chem. Phys. Lett.* 1995, *236*, 389-394.

49 Connelly, N. G.; Geiger, W. E. *Chem. Rev.*, 1996, *96*, 877-910.

50 The surface enhanced resonance Raman spectra recorded at 785 nm (see **Figure S5** in the SOI) are consistent with spectra obtained earlier for self-assembled monolayers.[36]

51 (a) Mizoguchi, T.; Adams, R. N. *J. Am. Chem. Soc.* 1962, *84*, 2058–2061 (b) Yang, H.; Wipf, D. O.; Bard, A. J. *J. Electroanal. Chem.* 1992, *331*, 913-924.

52 de Silva, A. P.; Uchiyama S. *Nat. Nanotechnol*. 2007, *2*, 399-410.